

# In vitro and biodistribution examinations of Tc-99m-labelled doxorubicin-loaded nanoparticles

Andras Polyak<sup>1</sup>, Elena Alina Palade<sup>2</sup>, Lajos Balogh<sup>1</sup>, Zita Postenyi<sup>1</sup>, Veronika Haasz<sup>1</sup>, Gergely Janoki<sup>3</sup>, Gyozo A. Janoki<sup>4</sup>

<sup>1</sup>National "F.J.C." Research Institute for Radiobiology and Radiohygiene (NRIRR), Budapest, Hungary

<sup>2</sup>Department of Pathology and Forensic Veterinary Medicine, Faculty of Veterinary Science, Szent István University, Budapest, Hungary

<sup>3</sup>Radiopharmacy Laboratories Ltd., Budapest, Hungary

<sup>4</sup>Medi-radiopharma Ltd., Budapest, Hungary

[Received 26 V 2011; Accepted 16 XI 2011]

## Abstract

**BACKGROUND:** Nanoparticles represent promising drug carrier systems. In the case of cytostatics such as doxorubicin, carrier colloid systems as human serum albumin (HSA) nanoparticles, may increase their therapeutic efficiency and decrease their side-effects (toxicity) and any potential multidrug resistance. In the present study, doxorubicin, as a widely used antineoplastic agent, was incorporated into the matrix of human serum albumin and three different particle-sized doxorubicin-loaded HSA nanoparticles were prepared, using a previously described desolvation method. Our objective was to find out if different particle sizes of colloid carriers can allow regarding the given cytostatic agent.

**MATERIAL AND METHODS:** The three prepared nanoparticles were labelled using technetium (Tc-99m) and were tested for their physicochemical colloidal quality, fluctuations, and radiochemical stability. Biodistribution of different-sized radiolabelled colloids were determined by means of scintigraphic imaging stu-

dies in healthy male Wistar rats. Images were taken by gamma camera at several times and organ uptakes were estimated by quantitative ROI analysis.

**RESULTS:** *In vitro* measurements showed that more than 95% of doxorubicin proportion was permanently adsorbed to human serum albumin. Radiolabelled doxorubicin-loaded particles had high-degree and durable labelling efficiency and particle size stability. Biodistribution results had a close correlation to earlier described results of radiocolloids in similar particle size ranges. *In vivo* examinations verified that colloid carriers have insignificant size fluctuations after an intravenous application and they show the proper distribution according to their particle size.

**CONCLUSIONS:** Our investigations verified that different and stable particle sizes make drug carrier HSA nanoparticles possible to apply different drug targeting in a potential clinical use.

**Key words:** doxorubicin, HSA, Tc-99m, nanoparticle, colloid, labelling, biodistribution

Nuclear Med Rev 2011; 14, 2: 55–62

## Introduction

In recent years new methods have been developed with nanoparticles as drug delivery systems (nanocarriers) in oncological applications to targeted delivery antineoplastic drugs. The use of colloidal carriers can decrease side-effects in treatment and increase therapeutic efficiency [1]. In cancer therapy doxorubicin is a frequently used antineoplastic agent, but in clinical applications this anti-cancer drug is limited due to its high cardiotoxicity [2, 3]. A promising solution to decrease cardiotoxicity could be binding doxorubicin to a drug delivery nanoparticle system [4]. Nanoparticles show a high drug loading efficiency with minor drug leakage, high storage stability, and may overcome cancer cell multidrug resistance [5, 6]. Earlier, doxorubicin was bound to colloidal carriers made from several agents such as poly(butyl cyanoacrylate) (PBCA) [7, 8], poly(isohexyl cyanoacrylate) (PIHCA) [9], poly(lactic-co-glycolic acid) (PLGA) [10], and gelatin [11, 12].

Doxorubicin-loaded colloids have benefits in comparison to the normal doxorubicin solutions: firstly, passive targeting due to

Correspondence to: Andras Polyak  
 National "F.J.C." Research Institute for Radiobiology and Radiohygiene (NRIRR)  
 Anna Str. 5, Budapest, Hungary, H-1221  
 e-mail: bandi.polyak@gmail.com

the enhanced permeation and retention effect (EPR effect, [13]) that results from the properly selected particle-size distribution, and secondly, elimination of the multidrug resistance in more cancer cell lines [14].

Several methods have been described for bounding drugs to nanoparticulate systems, such as surface attachment of drugs to nanoparticles or polymers [6, 15], adsorption to the preformed carrier system, and incorporation into the particle matrix during colloid preparation [4]. While simple adsorption to preformed carrier nanoparticles could lead to the early desorption of targeting ligand, incorporation protects drug-loaded particles from early drug loss, inactivation, or degradation during storage and after administration [4].

In the present study, doxorubicin was incorporated into the matrix of human serum albumin, and three different particle-sized fractions of doxorubicin-loaded HSA nanoparticles were prepared using a previously described desolvation method [16, 17]. HSA nanoparticles offer several specific advantages [16]: these colloid compounds are biodegradable and well-tolerated, preparation is easy and reproducible [17], and it is possible to bind targeting ligands to particles by covalent bonding, due to the presence of functional groups [18–21].

The attained nanoparticles were labelled with technetium (Tc-99m) and investigated for their physicochemical (doxorubicin-conjugating) radiochemical purity. Particle sizes and their stabilities and fluctuations were measured by dynamic light scattering, and examinations were reinforced by TEM images.

Different biodistributions of different sized radiocolloids were investigated in healthy Wistar rats. A previously designed protocol was applied to find out correlations with earlier biodistribution studies of comparable particle-sized nanoparticles [22–26]. Our further aim was to verify the lack of any incidental, too high particle-size fluctuations and degradation after intravenous injection.

## Material and methods

### Chemicals

Human serum albumin was obtained from C.A.F.-D.C.F. cvba-scr1 (albumin 20%), and glutaraldehyde 8% solution was obtained from Sigma (Steinheim, Germany). Doxorubicin (50 mg/25 ml doxorubicinum chloratum) and saline solution ("Salsol A", 0.9% w/v of NaCl) were from TEVA (Salsol A, Teva Pharmaceutical Works Ltd., Debrecen, Hungary). <sup>99m</sup>Tc-pertechnetate was derived from an UltraTechnekov (10.75 GBq) technetium generator (Covidien Imaging Solutions, USA). ACN (Acetonitrile) HPLC-grade was from Carlo Erba, and other solvents such as ethanol, MEK (Methyl Ethil Ketone), and all other reagents were purchased from Reanal Ltd. (Budapest, HU) and were of analytical grade. ITLC-SG was obtained from Pall Corporation. Chemicals for animal experiments, such as xylazine hydrochloride and ketamine hydrochloride, were obtained from CP-Pharma, Germany.

### Preparation and characterization of doxorubicin-loaded HSA nanoparticles

#### Preparation of different-sized, doxorubicin-loaded HSA nanoparticles

A total of 200  $\mu$ l of doxorubicin solution (1 mg/ml diluted doxorubicinum chloratum sol.) was added to 200  $\mu$ l (20 mg/ml)

HSA solution. As previously described, the pH value of this initial HSA solution can influence the resulting particle sizes [17]. Therefore, three different pH settings (pH = 6.2, pH = 7.5, and pH = 8.2) were used by adding 0.1 N HCl or 0.1 N NaOH. The three mixtures were incubated under 650 rpm stirring for 2 hours at room temperature to adsorb doxorubicin to human serum albumin [4, 27]. For the desolvation method 3 ml 96% v/v ethanol was added using a calibrated Masterflex tubing pump (Cole-Palmer Co., Chicago, Ill., USA) at 1 ml/min speed and continuous stirring (650 rpm). After the desolvation process, 10  $\mu$ l of 8% glutaraldehyde solution was added to induce particle crosslinking. This process was carried out under stirring (650 rpm) incubation for 24 hours at RT. Prepared nanoparticles were purified by centrifugation (16000 g, 8 min) and redispersion in phosphate buffer (pH = 7.5) by vortexer [27] and 5 minutes of ultrasonication [4].

#### Determination of non-adsorbed doxorubicin proportion

After centrifugation (16,000 g, 8 min) and redispersion in phosphate-buffer, the collected supernatants were used to determine the non-adsorbed doxorubicin ratio. For the quantification of doxorubicin in the supernatant samples, an Agilent 1200 HPLC system (Agilent Technologies Inc.) with UV-VIS detector was applied. A LiChroCART® 250-4 LiChrospher® 100 RP-18 reverse phase column (Merck, Germany) was used for the assay, and separation was achieved using an isocratic mixture of water and acetonitrile (7:3) containing 0.1% trifluoroacetic acid [28] at a flow rate of 0.8 ml/min. Doxorubicin was quantified by UV (250 nm), and the retention time was about 12 min [4]. Non-adsorbed doxorubicin quota was followed up 1 and 24 hours and 7 days after preparation. Samples were stored at RT in a dark place.

#### Characterization of particle size and colloid stability

Particle size and polydispersity of attained colloids were measured by dynamic light scattering using a Dynapro instrument (Proteinsolutions Inc., VA, USA) as described earlier [23]. Samples were diluted 1:10 with saline and were measured at room temperature. Colloidal stability of nanoparticles was followed up 1, 2, 8, and 24 hours and 2, 4, and 7 days after preparation. Samples were stored at RT in a dark place.

#### Transmission electron-microscopy examinations

Although particle fraction-ranges of the examined samples were near to the upper threshold of the measuring range for laser scattering instrument (6 microns), TEM examinations were carried out to verify that the particles were in the earlier determined ranges.

Doxorubicin-loaded HSA nanoparticle solutions were prepared according to the single-droplet negative staining technique [29] using carbon coated formvar copper grids and ammonium molybdate as a contrasting solution, and they were examined with a transmission electron-microscope (TEM) at various magnifications (JEOL, Japan). Pictures were taken with a MegaView III camera and processed with the Soft Imaging Systems analysis program.

### Labelling method and in vitro radiochemical stability

For labelling, 200  $\mu\text{g}$   $\text{SnCl}_2 \cdot (\text{x}2\text{H}_2\text{O})$  was added to 2 ml of Doxo-HSA-Colloid as a reducing agent, then 1 ml (1000 MBq activity) of generator-eluted  $^{99\text{m}}\text{TcO}_4^-$  (aqueous pertechnetate solution) was added to the solvent. Labelling was performed in 60 min incubation at RT [28]. Radiochemical purity was examined by means of thin layer chromatography, using silica gel as the coating substance on a glass-fibre sheet (ITLC-SG) [30]. Plates were developed in methyl ethyl ketone. We applied a Raytest MiniGita device (Mini Gamma Isotope Thin Layer Analyzer) in Radiopharmacy Ltd. to determine the distribution of radioactivity in the developed ITLC-SG plates. We examined labelling efficiency 1, 6, and 24 h after labelling. Radiochemical samples were stored at RT in a dark place.

### In vivo examinations, animal experiments

The aim of *in vivo* examinations was to observe particle-size changes or degradation after intravenous injection and to find out possible correlations with earlier presented biodistribution results of HSA colloids among the same size-ranges. These HSA products were earlier described in studies concerned with lymphoscintigraphy [23], lung scintigraphy [22], and other particle size-dependent biodistribution tests [25, 26].

The biological behaviour of different-sized colloids was ascertained by carrying out scintigraphic imaging studies in healthy male Wistar rats weighing 180–200 grams. Then 0.2 ml (120 MBq of  $^{99\text{m}}\text{Tc}$ ) of the radiolabelled colloids was administered through the tail vein of the animals. Dorso-ventral and left-lateral images were taken with a single-head digital SPECT gamma camera (Nucline X-ring, Mediso) at 5, 15, 30, and 60 minutes and 2, 8, and 22 hours post-injection using a LEHR collimator to determine the *in vivo* localization of injected radioactivity. Prior to the imaging the animals were anaesthetized by administering a combination of xylazine hydrochloride and ketamine hydrochloride intraperitoneal. The gamma camera was previously calibrated for the 140

keV gamma photon of  $^{99\text{m}}\text{Tc}$ . All the images were acquired with 60 second time-prerequisites using a  $1024 \times 1024 \times 16$  matrix size. Critical organs, e.g. heart, liver, spleen, shoulder (representing the bone marrow uptake), and urinary bladder, were drawn around and organ uptakes were estimated by quantitative ROI analysis.

All the animal experiments reported here were carried out in strict compliance with the relevant national laws of Hungary. This study was approved by the Institutional Ethical Board.

## Results

### Non-conjugated doxorubicin concentration

Quantification of doxorubicin in the supernatant samples showed that at 1.0 mg/ml doxorubicin concentration more than 95% of the drug was adsorbed to nanoparticles. Doxorubicin loading efficiency was examined 6, 24, and 48 h after biological application of labelled nanoparticles and each quantification showed that more than 95% of the doxorubicin remained bound to the HSA.

### Particle size measurements and colloid stability

For the radiolabelling experiments three samples were manufactured with different mean diameters (about 180, 430, and 1800 nm) and particle-size distributions at different initial pH settings in due course of preparation. Fractions of nanoparticles are illustrated in a common particle-size distribution histogram (Figure 1). Representative values of nanoparticle fractions are summarized in Table 1. Relatively high (35...45%) polydispersity values belong to mean diameters (MD) 180, 430, and 1800 nm.

Fluctuations of particle-sizes were followed up for 1 week and the average diameter, polydispersity, and fraction-range values were measured at different times. Results are summarized in Table 2 and illustrated in Figure 2. The diameter of the particles fluctuated within a 2% range, but changes were not unidirectional or trend-like. The 180 nm and 430 nm MD nanoparticles had 1.8%

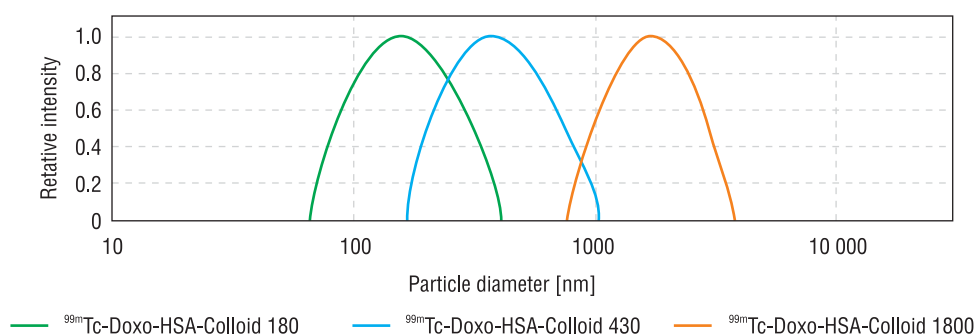


**Figure 1.** Particle-size distribution histogram of the three nanoparticle samples: maximum relative intensities were set to 1 to compare their size distribution in a common histogram.

**Table 1.** Representative values of nanoparticle-fractions measured immediately after preparation

No.	Sample	Mean diameter	Polydispersity	Total fraction range
1.	$^{99\text{m}}\text{Tc}$ -Doxo-HSA-Coll 180	176 nm	43.3%	65–405 nm
2.	$^{99\text{m}}\text{Tc}$ -Doxo-HSA-Coll 430	429 nm	44.1%	165–1044 nm
3.	$^{99\text{m}}\text{Tc}$ -Doxo-HSA-Coll 1800	1764 nm	35.5%	755–3762 nm

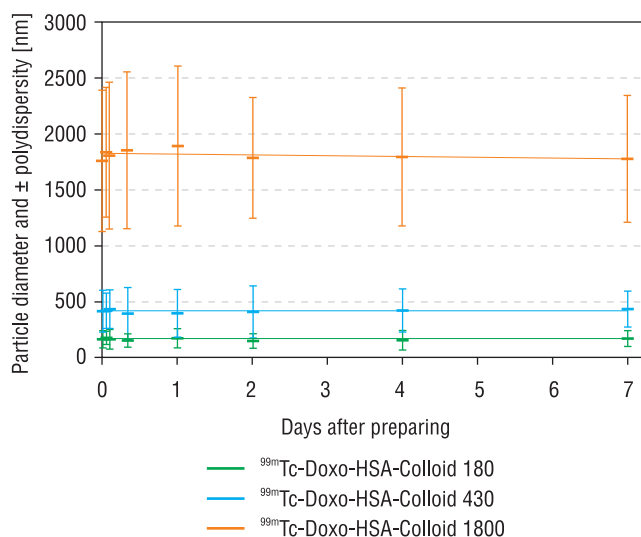


**Figure 2.** *In vitro* colloid size-stability examination of the different-sized doxorubicin-loaded nanoparticles: fluctuations of average diameter values with polydispersities (illustrated as  $\pm$  SD).

and 1.2% average particle-size growth, while the 1800 nm MD nanoparticles had 1.9% average diameter decrease during the follow-up. Thus doxorubicin-loaded nanoparticles showed a high degree of particle-size stability.

At different times, mean particle-diameters showed fluctuations with an  $\pm$  SD = 3.5...4.7%, but average particle size changes were insignificant during the 1<sup>st</sup> week (Table 2).

### TEM images of colloids

The TEM examination revealed the presence of mostly spherical-shaped particles (Figure 3). Each sample showed broad size-distribution, but each observed size of particles was in the previously determined particle-fraction ranges. Besides, we could not see any particles larger than 6 microns in the largest product (<sup>99m</sup>Tc-Doxo-HSA-Coll1800). It was important because the upper threshold of size-measuring in the applied laser scattering method was 6 microns. Thus, light scattering measurements were reinforced by TEM images.

### Labelling efficiency, radiochemical purity, and stability

Efficiency of Tc-99m binding was examined 1, 6, and 24 h after labelling. Radiochemical samples were stored at RT in a dark place. Measurements verified that 1 hour after labelling each colloid had at least 95% radiochemical efficiency and 6 and 24 h after labelling the products kept radiochemical stability. Measured labelling efficiencies even increased to 98...99% (Figure 4).

### In vivo examinations

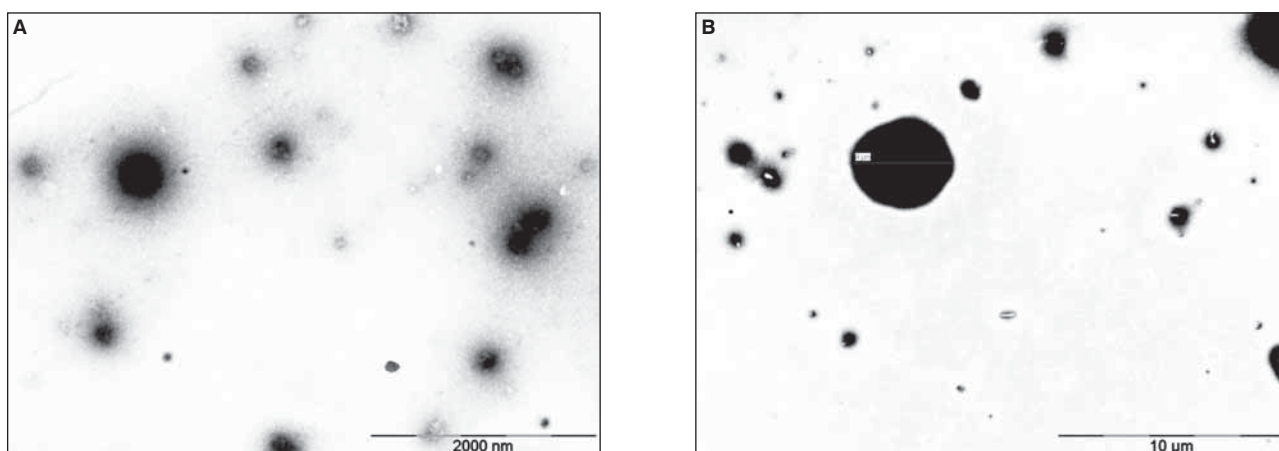
All the injected animals survived the experiments and no clinical side-effects (screaming, salivation, tremor, dyspnoe, diarrhoea, restlessness, or state of coma) were recorded in the rats. There was no sign of radioactivity in thyroid, salivary gland, or gastric mucosa at any time, indicating a high radioactive yield and stable *in vivo* labelling of all three agents.

The applied radiolabelled nanoparticles disappeared from the blood-stream relatively quickly. In the first 5 minutes post-ap-

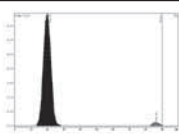
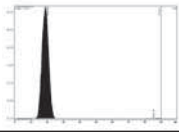
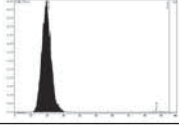
**Table 2.** Colloid stability in nanometre values: measured mean diameters ("Mean D") immediately after preparation ("T<sub>0</sub>" time point) with polydispersity values ("Polyd"), average, and  $\pm$  SD values during the 7 days of follow-up

	<sup>99m</sup> Tc-Doxo-HSA-Coll180		<sup>99m</sup> Tc-Doxo-HSA-Coll430		<sup>99m</sup> Tc-Doxo-HSA-Coll1800	
	Mean D [nm]	Polyd [nm]	Mean D [nm]	Polyd [nm]	Mean D [nm]	Polyd [nm]
T0 (starting)	175.8	76.1	429	189.3	1764	626.1
Average of 7 days	176	74.1	426.1	193.8	1817.7	623.8
$\pm$ SD of 7 days	8.3	11.9	14.6	26.9	39.3	60.3

SD — standard deviation



**Figure 3.** Transmission electron-micrographs of doxorubicin-loaded HSA nanoparticles. **A.** <sup>99m</sup>Tc-Doxo-HSA-Coll180; **B.** <sup>99m</sup>Tc-Doxo-HSA-Coll1800.

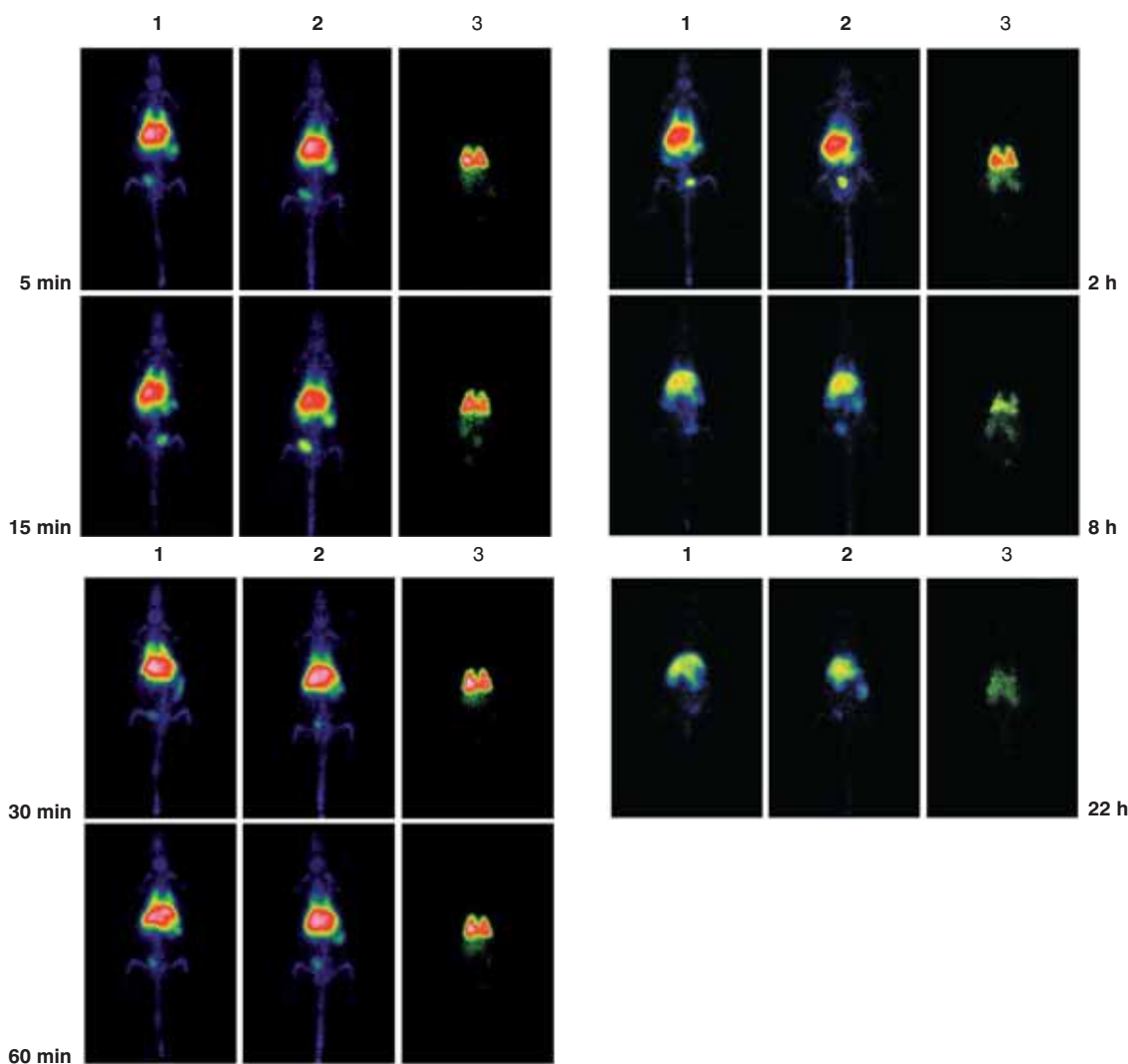
	Chromatogram	Substance	R/F	Area counts	Area (%)
1 h		Reg #1	0.000	21,930.09	97.37
		Reg #2	0.948	592.09	2.63
6 h		Reg #1	0.004	15,509.48	99.98
		Reg #2	0.939	592.09	0.02
24 h		Reg #1	0.009	17,140.33	99.88
		Reg #2	0.924	20.67	0.12

**Figure 4.** Radiochemical measurements of the  $^{99m}\text{Tc}$ -Doxo-HSA-Coll430 in ITLC-SG with Raytest MiniGita scanner, at different times: labelled nanocolloids are at starting point, free  $^{99m}\text{Tc}$ -pertechnetate runs with the front ( $R_f \approx 1$ ).

plication, no large vessels were visualized. The two smaller particles were quickly taken up by the RES organs (liver, spleen, bone marrow) and the accumulated radioactivity immediately started to wash-out through the urinary tract (kidneys, urinary bladder, urine). However, almost 80% of the applied greatest radiolabelled agent localized in the lungs, even on the first scans (Figure 5).

Only minor differences were recognized between the colloid particles No. 1 and 2 (average diameter 180 nm and 430 nm), respectively. Both radiocolloids were excreted in the same amount (nearly 50% in 22 hours post application) through the urinary tract of the animals.

The greater doxorubicin-loaded colloid ( $^{99m}\text{Tc}$ -Doxo-HSA-Coll 1800), however, markedly differed from the two smaller ones. The major proportion of radioactivity (78.6%) appeared in the lungs, much less but increasing and visible in the liver, and no appearance was documented in the scans in the spleen and skeleton (Table 3, Figure 6). The greater radiolabelled compounds located in the lungs disaggregated later, and the smaller particles re-located mainly in the liver (Table 3A, 3B, Figure 7). This is the explanation of the observation that the measured radioactivity

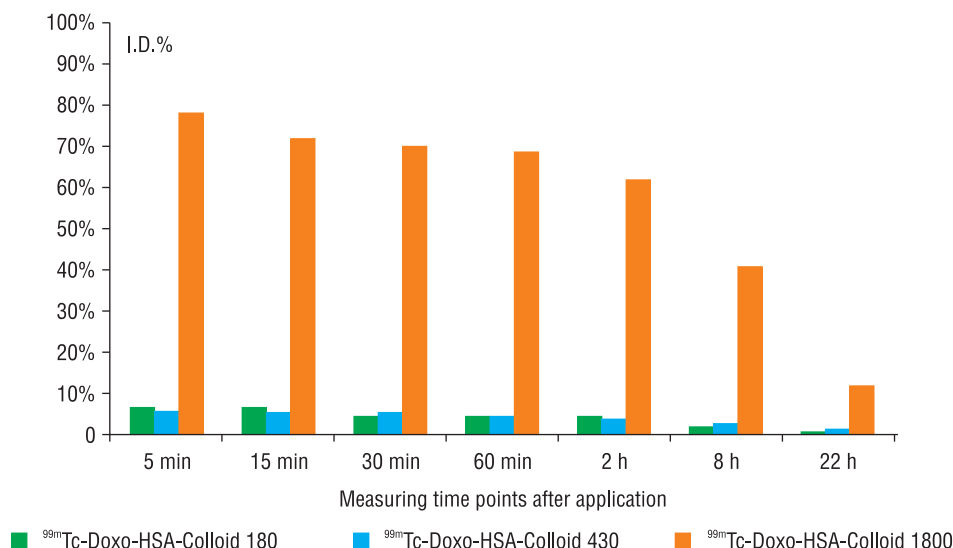


**Figure 5.** Ventrodorsal whole body scans of Wistar rats after intravenous application of different sized doxorubicin-loaded HSA nanoparticles. Injected dose was 60 MBq/200  $\mu\text{l}$ . 1:  $^{99m}\text{Tc}$ -Doxo-HSA-Coll180, 2:  $^{99m}\text{Tc}$ -Doxo-HSA-Coll430, 3:  $^{99m}\text{Tc}$ -Doxo-HSA-Coll1800.



**Table 3. Biodistribution of radiocolloids: summary of calculated % ID values of the three radiocolloids taken from ROI data of scan images. Measured counts were adjusted to initial time with the respective decay of Tc-99m isotope**

	5 min	15 min	30 min	60 min	2 h	8 h	22 h
<b><sup>99m</sup>Tc-Doxo-HSA-Coll180</b>							
Total	100.00%	95.70%	96.50%	93.80%	89.40%	74.30%	55.70%
Lungs	6.30%	6.20%	4.50%	4.30%	4.60%	2.50%	0.90%
Liver	72.50%	71.30%	68.40%	67.10%	63.80%	50.90%	37.10%
Spleen	2.20%	1.00%	2.40%	1.20%	2.80%	2.70%	1.40%
Kidneys	1.70%	1.90%	2.60%	1.70%	3.10%	5.60%	3.80%
Bladder	1.00%	1.20%	1.80%	0.70%	2.90%	1.90%	1.00%
Excreted radioactivity		4.30%	3.50%	6.20%	10.60%	25.70%	44.30%
<b><sup>99m</sup>Tc-Doxo-HSA-Coll430</b>							
Total	100.00%	99.10%	98.90%	97.20%	88.00%	71.90%	51.30%
Lungs	5.00%	5.20%	5.40%	4.90%	4.00%	3.20%	1.60%
Liver	73.90%	72.80%	70.10%	64.90%	59.70%	45.70%	31.40%
Spleen	1.70%	1.90%	2.00%	3.30%	4.00%	3.50%	3.50%
Kidneys	2.20%	2.10%	1.90%	4.70%	3.30%	3.80%	3.00%
Bladder	0.60%	1.50%	2.00%	4.70%	4.50%	2.50%	1.10%
Excreted radioactivity		0.90%	1.10%	2.80%	12.00%	28.10%	48.70%
<b><sup>99m</sup>Tc-Doxo-HSA-Coll1800</b>							
Total	100.00%	88.70%	89.60%	91.20%	91.40%	82.60%	71.80%
Lungs	78.60%	71.00%	68.90%	67.20%	61.20%	39.90%	12.00%
Liver	8.30%	9.40%	9.30%	11.20%	14.90%	22.50%	29.00%
Spleen	0.30%	0.60%	1.40%	1.70%	0.60%	1.70%	2.30%
Kidneys	0.70%	0.80%	1.00%	2.00%	1.20%	2.50%	2.00%
Bladder	0.10%	0.10%	0.20%	0.20%	0.10%	1.60%	0.80%
Excreted radioactivity		11.30%	10.40%	8.80%	8.60%	17.40%	28.20%

**Figure 6.** Injected dose percentage values in lungs after application.

in the lungs decreased approximately by the same amount as it increased at that time in the liver. Only 28% of administered radioactivity excreted via the urinary tract in 22 hours post application (Figure 8).

Biodistributions showed close correlation to earlier pharmacokinetic studies [22–26] of other HSA products. The different uptakes of lungs and liver verified that different particle-diameters did not change significantly immediately

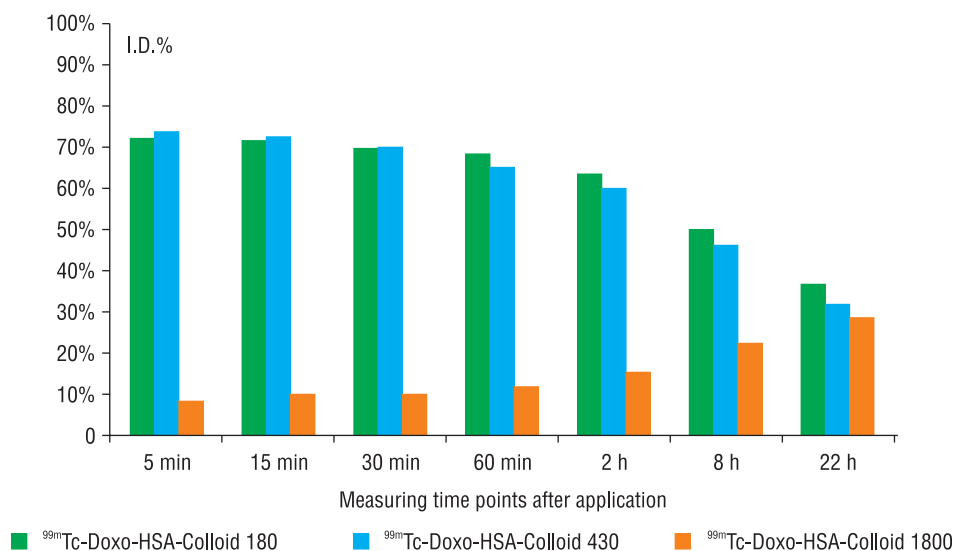


**Figure 7.** Injected dose percentage values in liver after application.

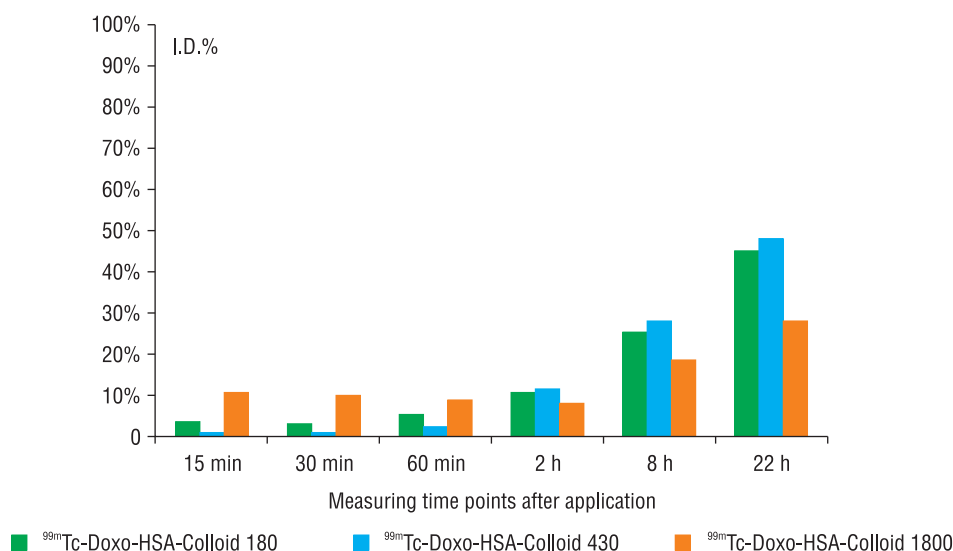


**Figure 8.** Excreted activity ratio values after application.

after intravenous injection and particles did not disaggregate. However, 6 hours and almost 1 day after IV application, colloid agents showed the proper distribution according to their particle size and less than 50% of injected activity excreted through the urinary tract.

## Discussion

The present study demonstrates the preparation and investigation of doxorubicin-loaded HSA nanoparticles in different particle-sizes. Three samples, different by means of particle-size distribution and fraction-range, were considered for the experiments. Non-adsorbed doxorubicin quota was checked and followed-up respectively, until 7 days after preparation, and verified that more than 95% of doxorubicin proportion was permanently adsorbed to human serum albumin.

The prepared doxorubicin-loaded particles were radiolabelled by  $^{99m}\text{Tc}$  with high-degree and durable labelling efficiency as the *in vitro* radiochemical stability measurements demonstrates. Another aspect is the size stability: particle size was observed for 1 week. Each product showed a high degree of colloid size-stability: diameters and polydispersities of particle fractions fluctuated within a relatively narrow range and changes were not unidirectional, nor trend-like.

The different biological behaviours of the different-sized colloids were examined by scintigraphic imaging studies in healthy male Wistar rats. Ventrodorsal and left-lateral images were taken with a digital SPECT gamma camera at different times till 22 h post injection and organ uptakes were estimated by quantitative ROI analysis. The *in vivo* biodistribution data of doxorubicin-loaded radiocolloids had a very close correlation to earlier described results [22–26]. Images and calculated injected dose percentage values em-

phasized that directly post-injection, the greatest particle-sized compounds were located especially in the lungs and they slowly disaggregated. The smaller particle fractions were relocated mainly in the liver and they also had slow elimination. Our investigations verified that application of different particle sized doxorubicin-loaded HSA nanoparticles make drug carrier systems possible to apply different drug targeting in potential clinical use.

## Acknowledgments

This scientific work was supported by several national (OTKA-68376, JEDIONKO, KMOP-1.1.1-08/1-2008-0017, GOP-1.1.1.-09/1-2010-0107) and international (IAEA-CRPs, EMIL NoE) projects.

## References

- Mishra B, Patel BB, Tiwari S. Colloidal nanocarriers, a review on formulation technology, types and applications toward targeted drug delivery. *Nanomedicine: Nanotechnology, Biology and Medicine* 2010; 6: 9–24.
- Singal PK, Li T, Kumar D, Danelisen I, Iliksovic N. Adriamycin-induced heart failure: mechanism and modulation. *Mol Cell Biochem* 2000; 207: 77–86.
- Minotti G, Menna P, Salvatorelli E, Cairo G, Gianni L. Anthracyclines: molecular advances and pharmacologic developments in antitumor activity and cardiotoxicity. *Pharmacol Rev* 2004; 56: 185–229.
- Dreis S, Rothweiler F, Michaelis M, Cinatl J Jr, Kreuter J, Langer K. Preparation, characterization and maintenance of drug efficacy of doxorubicin-loaded human serum albumin (HSA) nanoparticles HSA. *International Journal of Pharmaceutics* 2007; 341: 207–214.
- Cuvier C, Roblot-Treupel L, Millot JM et al. Doxorubicin-loaded nanoparticles bypass tumor cell multidrug resistance. *Biochem Pharmacol* 1992; 44: 509–517.
- Cho K, Wang X, Nie S, Chen ZG, Shin DM. Therapeutic nanoparticles for drug delivery in cancer. *Clin Cancer Res* 2008; 14: 1310–1316.
- Gulyaev AE, Gelperina SE, Skidan IN, Antropov AS, Kivman GY, Kreuter J. Significant transport of doxorubicin into the brain with polysorbate 80-coated nanoparticles. *Pharm Res* 1999; 16: 1564–1569.
- Steiniger SC, Kreuter J, Khalansky AS et al. Chemotherapy of glioblastoma in rats using doxorubicin-loaded nanoparticles. *Int J Cancer* 2004; 109: 759–767.
- Cuvier C, Roblot-Treupel L, Millot JM et al. Doxorubicin-loaded nanoparticles bypass tumor cell multidrug resistance. *Biochem Pharmacol* 1992; 44: 509–517.
- Yoo HS, Oh JE, Lee KH, Park TG. Biodegradable nanoparticles containing doxorubicin-PLGA conjugate for sustained release. *Pharm Res* 1999; 16: 1114–1118.
- Leo E, Vandelli MA, Cameroni R, Forni F. Doxorubicin-loaded gelatin nanoparticles stabilized by glutaraldehyde: Involvement of the drug in the cross-linking process. *Int J Pharm* 1997; 155: 75–82.
- Leo E, Cameroni R, Forni F. Dynamic dialysis for the drug release evaluation from doxorubicin-gelatin nanoparticle conjugates. *Int J Pharm* 1999; 180: 23–30.
- Maeda H, Wu J, Sawa T, Matsumura Y, Hori K. Tumor vascular permeability and the EPR effect in macromolecular therapeutics: a review. *J Control Rel* 2000; 65: 271–284.
- Barraud L, Merle P, Soma E et al. Increase of doxorubicin sensitivity by doxorubicin-loading into nanoparticles for hepatocellular carcinoma cells in vitro and in vivo. *J Hepatol* 2005; 42: 736–743.
- Eatock M, Church N, Harris R et al. Activity of doxorubicin covalently bound to a novel human serum albumin microcapsule. *Invest New Drugs* 1999; 17: 111–120.
- Weber C, Coester C, Kreuter J, Langer K. Desolvation process and surface characterisation of protein nanoparticles. *Int J Pharm* 2000; 194: 91–102.
- Langer K, Balthasar S, Vogel V, Dinauer N, von Briesen H, Schubert D. Optimization of the preparation process for human serum albumin (HSA) nanoparticles. *Int J Pharm* 2003; 257: 169–180.
- Nobs L, Buchegger F, Gurny R, Allemann E. Current methods for attaching targeting ligands to liposomes and nanoparticles. *J Pharm Sci* 2004; 93: 1980–1992.
- Wartlick H, Michaelis K, Balthasar S, Strebhardt K, Kreuter J, Langer K. Highly specific HER2-mediated cellular uptake of antibody-modified nanoparticles in tumour cells. *J Drug Target* 2004; 12: 461–471.
- Dinauer N, Balthasar S, Weber C, Kreuter J, Langer K, von Briesen H. Selective targeting of antibody-conjugated nanoparticles to leukemic cells and primary T-lymphocytes. *Biomaterials* 2005; 29: 5898–5906.
- Steinhauser I, Spänkuch B, Strebhardt K, Langer K. Trastuzumab-modified nanoparticles: optimisation of preparation and uptake in cancer cells. *Biomaterials* 2006; 28: 4975–4983.
- Arshady R. *Microspheres, microcapsules & liposomes*. Citus Books, London 2001.
- Mirzaei S, Rodrigues M, Hoffmann B et al. Sentinel lymph node detection with large human serum albumin colloid particles in breast cancer. *Eur J Nucl Med Molec Imag* 2003; 30: 868–873.
- Reddy LH, Sharma RK, Chuttani K, Mishra AK, Murthy RSR. Influence of administration route on tumor uptake and biodistribution of etoposide loaded solid lipid nanoparticles in Dalton's lymphoma tumor bearing mice. *J Controlled Release* 2005; 105: 185–198.
- Iliuma L, Davis SS, Wilson CG, Thomas NW, Frier M, Hardy JG. Blood clearance and organ deposition of intravenously administered colloidal particles. The effects of particle size, nature and shape. *International J Pharm* 1982; 12: 135–146.
- Whateley TL, Steele G. Particle size and surface charge studies of a tin colloid radiopharmaceutical for liver scintigraphy. *Eur J Nucl Med* 1985; 10: 353.
- Wagner S, Rothweiler F, Anhorn MG et al. Enhanced drug targeting by attachment of an anti  $\alpha v$  integrin antibody to doxorubicin loaded human serum albumin nanoparticles. *Biomaterials* 2010; 31: 2388–2398.
- Configliacchi E, Razzano G, Rizzo V, Vigevani A. HPLC methods for the determination of bound and free doxorubicin, and of bound and free galactosamine, in methacrylamide polymer-drug conjugates. *J Pharm Biomed Anal* 1996; 15: 123–129.
- Harris JR, Reiber A. Influence of saline and pH on collagen type I fibrillogenesis in vitro: Fibril polymorphism and colloidal gold labeling. *Micron* 2007; 38: 513–521.
- European Pharmacopoeia 6.0, 1029–1030.